Predicting interband transition energies for InAs/GaSb superlattices using the empirical pseudopotential method

Rita Magri
Istituto Nazionale per la Fisica della Materia, S[3], and Dipartimento di Fisica Universitá di Modena e Reggio Emilia, Via Campi 213/A, Modena, Italy

Alex Zunger
National Renewable Energy Laboratory, Golden, Colorado 80401, USA
(Received 23 April 2003; published 27 October 2003)

Recent measurements surprisingly show that the lowest valence-to-conduction confined transitions in narrow $(InAs)_8/(GaSb)_n$ and $(InAs)_6/(GaSb)_n$ superlattices *increase* in energy as the barrier thickness n increases. We show that in addition to the mesoscopic geometric quantities (well and barrier sizes), an atomic-scale description of interdiffused interfaces is needed to correctly reproduce the observed spectroscopic trend. The interdiffused interface is modeled via diffusion equations. We compare our atomistic empirical pseudopotential calculation in which only the *bulk binary* data are fit to experiment, with contemporary methods in which agreement with experiment is forced using ideally abrupt interfaces.

DOI: 10.1103/PhysRevB.68.155329 PACS number(s): 73.21.Cd, 71.55.Eq, 71.20.Nr

I. INTRODUCTION: THE NEED FOR BOTH MESOSCOPIC AND ATOMISTIC MODELING OF NANOSTRUCTURE ELECTRONIC PROPERTIES

The use of quantum wells and superlattices in optoelectronics is predicated on designing confined energy levels with given separations. These energies depend both on mesoscopic conditions (e.g., geometric dimensions on a scale of ≈ 100 Å) and on atomistic details (e.g., interfacial segregation and interdiffusion on a scale of ≈ 5 Å). The dependence on atomic-scale properties is evident, for example, by significant changes in interband energies for nominally identical quantum systems grown at two different temperatures. For example, Yang *et al.*[1] found a 30–40 meV increase of a ≈ 300 meV band gap of a $(InAs)_{5.5}/(In_{0.28}Ga_{0.72}Sb)_{10}/(InAs)_{5.5}/(AlSb)_{14}$ structure, when the layer thicknesses were kept constant but the growth temperature of the device was increased from 460 to 500°C. This suggests that interdiffusion changes the band gap. Also, Vurgaftman, Meyer, and Ram-Mohan[2] showed that there are conspicuous differences in the band gap values as large as 100 meV for structures nominally identical. Bennett *et al.*[3] measured the band gaps of InAs/GaSb superlattices with almost pure InSb-like or GaAs-like interfaces and found a difference of 40 meV for superlattices with nominal period $n=8$. In particular, gaps $E_g = 209$ meV and 216 meV have been measured for two samples with In-Sb-like interfaces whereas a gap $E_g = 253$ meV was measured for a sample with only GaAs-like interfaces. The relative energy differences (about 40 meV) are enormous. Clearly, the atomic-level structure at the interface controls much of the band gap.

The theoretical question is which structural degrees of freedom need to be used to model the energy levels of quantum structures. The traditional approach is based on modeling only the mesoscopic scale features with abrupt interfaces, and predicting the ensuing energy levels.[4,5] Often disagreement with experiment is rectified by readjustment of energy band parameters while maintaining abrupt interface calculation.[6,7] However, interfacial interdiffusion is an experimental fact. For example, recent cross-sectional scanning tunneling microscopy measurements on InAs/InGaSb superlattices have indeed observed Sb penetration into InAs and As penetration into the first few layers of InGaSb.[8]

Interfacial effects are particularly important in the GaSb/InAs system because relatively narrow quantum wells are needed. This is so because the conduction band minimum (CBM) of bulk InAs is below the valence-band maximum (VBM) of bulk GaSb; this negative gap can be increased to a desired positive value by making the layers thin enough, thus pushing the CBM up and the VBM down. As a result, quantum structures with 4–20 monolayer well width are commonly studied. There is another reason why interfacial effects are important in this system, namely, the exceptionally low point-group symmetry of the ideal, abrupt interface. Indeed the absence of a common-atom in InAs/GaSb *geometrically mandates* that (001) heterostructures will have four (not two) types of bonds. For example, the interface formed from InAs-on-GaSb (which is conventionally referred to as normal interface) in the ideal situation of absence of interfacial atomic intermixing has the layer sequence

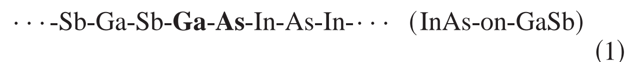
$$\cdots\text{-Sb-Ga-Sb-}\mathbf{Ga\text{-}As}\text{-In-As-In-}\cdots \quad \text{(InAs-on-GaSb)} \tag{1}$$

with an interfacial Ga-As bond, whereas the GaSb-on-InAs interface (the inverted interface) has the layer sequence

$$\cdots\text{-As-In-As-}\mathbf{In\text{-}Sb}\text{-Ga-Sb-Ga}\cdots \quad \text{(GaSb-on-InAs)} \tag{2}$$

with an In-Sb bond. Thus, not only In-As and Ga-Sb bonds are present, but also Ga-As and In-Sb bonds. This distinguishes these systems from common-atom heterostructures such as InAs/GaAs where only the bonds present in the binary constituents are present in the heterostructure. The geometric consequence of Eqs. (1) and (2) is that the point-group symmetry is reduced from D_{2d} common atom (InAs/GaAs) to C_{2v} no-common atom (InAs/GaSb). The optical

0163-1829/2003/68(15)/155329(8)/$20.00 ©2003 The American Physical Society

consequence is that in C_{2v} the valence-to-conduction transitions have a different matrix element in the two in-plane directions [110] and [−110], i.e., the in-plane polarization ratio, $\lambda=(P_{110}-P_{-110})/(P_{110}+P_{-110})$ (P being dipole matrix element), is different from 1. Such anisotropy was seen experimentally in high quality no-common atom superlattices (SL's), e.g., GaInAs/InP and AlInAs/InP.[9] Other consequences of the C_{2v} symmetry are the existence of finite couplings even at the Brillouin-zone center. This has a number of effects on the electronic structure and the optical properties. First, it leads to the appearance of parity *forbidden* $lh1 \leftrightarrow e2$ and $hh2 \leftrightarrow e1$ transitions).[10] Second, it causes energy-band anticrossings and subsequent shifts of the transition energies that are easily observed for given superlattice periods.[11] Third, it causes also the $e1 \leftrightarrow hh1$ and $e1 \leftrightarrow lh1$ transitions to develop an in-plane polarization anisotropy whereby the dipole transitions have unequal strength along the [110] and [−110] in-plane directions.[9] These C_{2v}-mandated optical properties are naturally sensitive to the symmetry and structure of the interfaces, so treating atomistic interfaces may be important.

In this paper, we describe a method for band-structure calculation based on an atomistic empirical pseudopotential method. Our approach describes the electronic charge distribution at the Ga-As and In-Sb interfaces and the band lineup readjustments of the superlattice components, interfaces included, with hydrostatic and/or biaxial strains. The effects of the local strains on the band structure are taken into account as well. We use our previous approach[12] of modeling the atomic structure of segregated interfaces by solving the kinetic diffusion equations. The resulting atomic structure is then used as input to an electronic structure calculation. We compare the results for the interband transition energies obtained with our method with those produced by other empirical pseudopotential methods (EPM) recently proposed. We show that to explain the experiment it is necessary to take into account segregation and interdiffusion at the interfaces.

II. THEORETICAL REQUIREMENTS FOR ATOMISTIC MODELING

In selecting an appropriate theoretical approach for describing quantum structures atomistically, and in particular the InAs/GaSb system, one has to bear in mind a few basic features.

First, in the no-common atom case one must theoretically account for four distinct bonds. The widely used theoretical approach to describe superlattice and multi-quantum-well band structure is the $\mathbf{k}\cdot\mathbf{p}$ and the envelope function approximation (EFA).[4] However, it has been pointed out by us[13] that, mostly because of the oversimplified description of the interfaces, the standard implementation of the $\mathbf{k}\cdot\mathbf{p}$-EFA approach is "farsighted" in that it does not recognize the proper superlattice symmetry, confusing it with a much higher symmetry. Among its deficiencies are the neglect of the correct C_{2v} symmetry of the (001) interfaces[14] and the ensuing heavy-light hole mixings at the Brillouin-zone center responsible for the optical in-plane polarization anisotropy.[9] Atomistic interfacial interdiffusion are also neglected in the standard $\mathbf{k}\cdot\mathbf{p}$ approach.[4] Other than for symmetry issues the EFA also assumes only In-As and Ga-Sb bonds in the system. But different bonds at the interfaces are necessary in order to obtain a different heavy-hole localization at the two In-Sb and Ga-As interfaces in agreement with what has been found in *ab initio* calculations for InAs/AlSb (001) superlattices.[15]

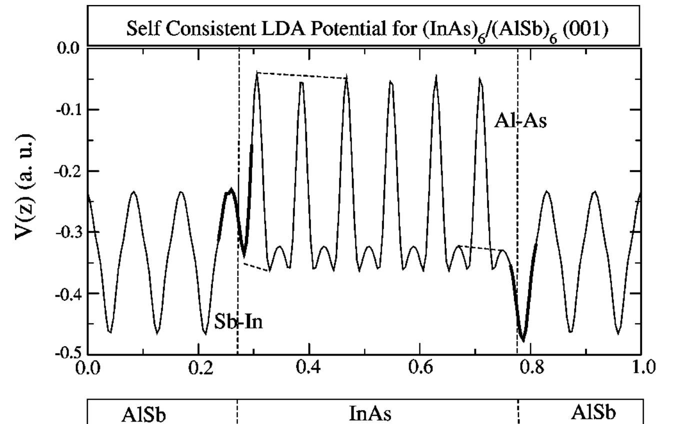

FIG. 1. (a) Self-consistent LDA total potential for the (001) $(InAs)_6/(AlSb)_6$ superlattice in atomic units. The calculation has been performed in a plane-wave basis using Trouiller-Martins pseudopotentials, a plane-wave cutoff of 22 Ry and exchange and correlation energy as proposed by Ceperley-Alder (Ref. 29) and parametrized by Perdew and Zunger (Ref. 30). Note that the InAs potential is different for different InAs layers. Similarly, the two interfaces have different potentials (bold solid lines).

Second, since we are dealing with rather short-period superlattices, the distance of a given layer from the interfaces will determine the potential at that layer. Thus, InAs monolayers that are distant from the interface may feel a bulk-like InAs potential, yet InAs monolayers closer to the interface will feel a surface-modified potential. This effect is evident if one examines the in-plane averaged, *self-consistent* potential we have obtained in *ab initio* local-density approximation (LDA) calculations. Figure 1 shows such a result for $(InAs)_6/(AlSb)_6$ (001) SL. The thin lines denote the in-plane (X-Y) averaged potential $\bar{V}(z)$, whereas the bold line emphasizes the potential at the two different interfaces. Close examination shows that (i) $\bar{V}(z)$ is different for the InAs monolayers (note the dashed lines) closest to the interface region, and (ii) the potential at the interfaces is different from those inside the respective layers (note bold lines). Unfortunately, self-consistent calculations such as that shown in Fig. 1 are not always practical computationally for large interdiffused superlattices (our calculations reported below require up to 1600 atoms per cell). In addition, even when practical, the LDA produces severely incorrect band gaps and large errors in the effective masses, both being detrimental to a realistic description of a nanostructure. Nevertheless, the unavoidable consequence of the self-consistent charge-transfer effects evident from *ab initio* calculations is that an appropriate theory must allow for different effective potentials (even for chemically identical monolayers) depending on the distance to the interfaces and also describe properly

the potential features at the two different interfacial bonds.

Third, whereas in bulk solids the effective potential form factors $V(\mathbf{G})$ are defined only for *bulk* reciprocal-lattice vectors $\mathbf{G}_{BK}$, in *superlattices* there are nonzero values of the potential also for the reciprocal-lattice vectors $\mathbf{G}_{SL}$ that are absent in the bulk. Some of these $\mathbf{G}_{SL}$ vectors have very small length in the case of nanostructures with very large unit cells. The values $\{V(\mathbf{q})\}$ for $\mathbf{q}\neq\mathbf{G}_{BK}$ are unimportant for the bulk solids, but control the band structure of lower-symmetry structures, such as superlattices or random alloys. Thus, an appropriate theory of InAs/GaSb SL's must determine, in some physical manner, $V(\mathbf{q})$ for $\mathbf{q}\neq\mathbf{G}_{BK}$.

Fourth, an ideal approach should easily describe superlattice interfacial segregation and intermixing, different strain situations (i.e., growth on different substrates), and the presence of alloys as superlattice constituents without the need to use different parameters or fit additional experimental data.

A number of recent calculation methods responded to the four challenges posed above, all assuming abrupt interfaces.

Recently, Dente and Tilton[6,16] (DT) applied a nonatomistic EPM to InAs/GaSb. In their approach the superlattice Hamiltonian is constructed from the potential form factors of the InAs and GaSb bulk constituents as in the approach of Xia.[17] The potentials of the two bulk constituents are *matched* continuously at the interfaces so there are no In-Sb or Ga-As bonds at the interface. The matching is done by using a rectangle function, centered on the interface and having the superlattice periodicity. The rectangle function is then expanded in a finite Fourier series on the superlattice reciprocal-lattice vectors, generating in this way the necessary $\mathbf{q}\neq\mathbf{G}_{BK}$ values. The number of Fourier components included in the expansion allows one to alter the sharpness of the interfaces. The epitaxial strain (i.e., InAs grown coherently on GaSb) is described only for the InAs bulk compound by changing the form factors of the reciprocal-lattice vectors whose squared magnitude is 3 $(2\pi/a)$ (mag-3) to fit the measured hydrostatic change in bulk band gap. The magnitude of some of the asymmetrical form factors corresponding to reciprocal-lattice vectors of squared magnitude $4\times(2\pi/a)$, (mag-4) is changed by introducing an additional parameter determined by fitting the light-hole-to-heavy-hole splitting under biaxial strain. No changes are made to other potential form factors.

Concerning the four theoretical requirements posed above, we note the following.

(i) Much like the $\mathbf{k}\cdot\mathbf{p}$, the approach of DT ignores the existence of interfacial bonds in a no-common atom SL, assuming instead that the InAs potential reaches to the interface, at which point the GaSb potential starts. Since no Ga-As and In-Sb bonds exist, this leads to the incorrect point-group symmetry (D_{2d}, rather than C_{2v}) and to an incorrect in-plane polarization ratio $\lambda=1$.

(ii) DT assume that the potential of all InAs monolayers are equal to each other, irrespective of the distance to the interface, and so are the potentials of all GaSb monolayers (see Fig. 1 of Ref. 16). This requires some unusual charge redistribution whose existence is not supported by self-consistent *ab initio* calculations (see Fig. 1).

(iii) The potentials $V(\mathbf{q})$ at $\mathbf{q}\neq\mathbf{G}_{BK}$ that are *required* by the SL's calculations are determined in the work of DT by implicitly selecting the rectangle function rect(z/w) (see Eq. (1) in Ref. 16) centered on the interface. But, since the interface bonds are not described, the interface region [at least two atomic layers in ideally stacked, no-common-atom (001) superlattices] becomes just a single layer, which is not physical. Moreover, their procedure introduces some uncontrolled elements: the specification of the number of Fourier components and origin of this function is equivalent to a significant set of parameters that needs somehow to be fixed. Given the way in which they build $\mathbf{G}$ for the superlattices, their approach cannot be readily extended to alloy superstructures.

(iv) This approach requires different sets of potential form factors (fit parameters) for each strain condition. Thus, small differences in an alloy constituent composition or strain conditions requires that a different fit is made in order to obtain a different set of form-factor parameters.

Another EP approach for InAs/GaSb system has been proposed in Refs. 18–20. They also have dealt with the description of strain effects. As in the case of the approach of Dente and Tilton, the effects of strain ϵ are included only in the description of the band structure of the *binary bulk* constituents. The form factors $V(\mathbf{G}_{BK},\bar{\epsilon})$ corresponding to a given strain $\bar{\epsilon}$ are obtained by fitting the deformation potentials at the Γ, X, and L points of the hydrostatically compressed or expanded bulk compounds. To treat intermediate strain, the form factors are interpolated between the values $V(\mathbf{G}_{BK},0)$ of the unstrained compounds and the fitted values $V(\mathbf{G}_{BK},\bar{\epsilon})$ of the strained compounds, allowing also for the corresponding change of $\mathbf{G}$ vector length. Unlike DT, in the approach of Refs. 18–20, all six form factors $V(\mathbf{G}_{BK})$ are allowed to change. To describe the potential of a superlattice strained layer, the atomic form factors of the corresponding strained bulk compound are interpolated at the intermediate $\mathbf{G}$ vectors of the superlattice reciprocal lattice. The potential of the In-Sb and Ga-As interfacial bonds are obtained using the form-factor values that describe the strained bulk InAs and GaSb compounds. Thus, the superlattice symmetry is taken into account properly but the description of the interface bonds themselves is only approximate since the chemical and strain properties of the In-Sb and Ga-As bonds are extracted using the atomic potentials appropriate to other compounds. No specific interface band offsets are used for the In-Sb and Ga-As interface bonds either. The approach of Refs. 18–20 is not easily extended to disordered superlattice configurations or alloy systems: perturbation theory is used for treating interfacial disorder effects and the virtual-crystal approximation for describing alloy components.

III. PRESENT METHOD

We solve the single-particle Schrödinger equation:

$$\left[-\frac{\beta}{2}\nabla^2+\sum_{n\alpha} v_{\alpha}(r-R_{n\alpha})\right]\psi_i(r)=\epsilon_i\psi_i(r), \tag{3}$$

where $R_{n\alpha}$ denotes the position of the nth ion of type α (= In, Ga, As, Sb) to obtain wave funtions and eigenvalues. The correct point-group symmetry is assumed by speci-

fying $R_{n\alpha}$. The term β, which scales the kinetic energy in the Schrödinger equation, has been introduced to represent the quasiparticle nonlocal self-energy effects.[14] In fact it can be shown that at the lowest order, the leading effects of the nonlocal many-body potential can be represented by scaling the kinetic energy.[21] This kinetic-energy scaling is needed to simultaneously fit bulk effective masses and band gaps. The crystal potential is written as a superposition of atomic potentials v_α centered around the atomic sites. The potential includes the spin-orbit interaction, thus the wave functions $\psi_i(r)$ are spinors with spin-up and spin-down components.

For the atomic potential v_α we use atomic screened pseudopotentials whose Fourier transform are continuous functions of momentum[22] $\mathbf{q}$. The functions $v_\alpha(\mathbf{q})$ are determined for each atomic species $\alpha=$Ga, Sb, In, As of the quaternary GaSb/InAs system. To obtain the values of the form factors at the intermediate $\mathbf{G}$ vectors appropriate for a given superstructure we need simply to evaluate the $v_\alpha(\mathbf{q})$ functions at the required $\mathbf{q}=\mathbf{G}$. The parameters entering the expression of the form factors are fitted to the experimentally measured electron and hole effective masses,[23] band gaps (target values at 0 K),[23] spin-orbit splittings,[23] hydrostatic deformation potentials of the band gaps,[23] band offsets,[23] and LDA-predicted single band-edge deformation potentials[24] of the four *binary* systems. The results of the fit are given elsewhere.[25]

To obtain the correct behavior of the band-edge energies under hydrostatic or biaxial strain deformations we have built the response to the strain directly into the screened atomic pseudopotentials v_α, adding an explicit strain dependent term $\delta v_\alpha(\epsilon)$. This term plays a crucial role in describing the variation of the valence-band edge and, separately, the conduction-band edge under arbitrary strains. This allows us to describe the modification of the valence- and conduction-band offsets when the systems are subjected to hydrostatic or biaxial deformation conditions such as in the case of epitaxial growth on a lattice-mismatched substrate. We fitted not only the experimental hydrostatic deformation potentials of the band gap, but also the *ab initio* calculated hydrostatic deformation potentials of the valence-band maximum.[24] Even though the binary GaSb and InAs systems are nearly lattice-matched (the lattice mismatch is relatively small, 0.6%), the interface Ga-As and In-Sb bonds are strongly deformed (their lattice mismatch with InAs and GaSb is about 6–7%) when the InAs/GaSb superlattices are grown on a GaSb (or InAs) substrate. Our scheme takes into account automatically the change in the valence-and conduction-band offsets of each constituent, including the interface bonds, due to changes in the biaxial constraints or local bonding deformations without the need to readjust any parameter. As a consequence, the heavy-hole wave function we calculate for the InAs/GaSb (001) superlattice has a much larger amplitude on the In-Sb interface bond than on the Ga-As bonds (see Ref. 25) in agreement with the results of *ab initio* calculations[15] as we also show in Fig. 2. Figure 2 shows a direct comparison between the heavy-hole charge density of a $(\mathrm{GaSb})_5/(\mathrm{InAs})_5$ superlattice integrated over the Brillouin zone (i.e., calculated and summed over the special k points) obtained from an *ab initio* calculation (in this case it is the self-consistent charge density) [Fig. 2(b)] and from the current atomistic empirical pseudopotential [Fig. 2(a)]. From this comparison we see that our empirical pseudopotential is able to reproduce the charge redistribution along the superlattice growth direction and at the two different In-Sb and Ga-As interfaces that can be obtained using an *ab initio* self-consistent approach.

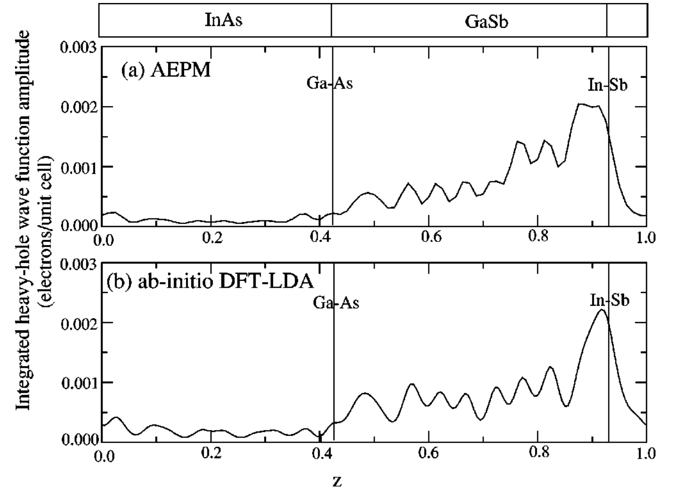

FIG. 2. Integrated heavy-hole ($hh1$) charge-density distribution of an $(\mathrm{InAs})_5/(\mathrm{GaSb})_5$ superlattice along the growth (z) direction calculated with: (a) the atomistic empirical pseudopotential approach (AEPM) and (b) the self-consistent *ab initio* DFT (density functional theory)-LDA approach.

To apply our scheme to different atomic local environments than those present in the fitted pure binary compounds we make the hypothesis that the charge redistribution around an atom depends only on its first neighbor shell. This seems to be a relatively good guess if we look at Fig. 1 where the *ab initio* self-consistent local potential features of the $(\mathrm{InAs})_6/(\mathrm{AlSb})_6$ superlattice is shown. The perturbation due to the interface affects mostly the potential of the atoms closest to the interface. In the quaternary $(AC)(BD)$ systems, the C and D anions can be surrounded by A_nB_{4-n} cations, where $n=0$, 1, 2, 3, and 4. Analogously, the A and B cations can be surrounded by C_nD_{4-n} anions. Our EPM has been obtained by fitting the properties of only the pure binary compounds (corresponding to environments $n=0$ and $n=4$). To improve the transferability to other environments, we assume a linear interpolation between these limits as

$$
\begin{aligned}
v_{\mathrm{A}}(C_nD_{4-n}) &= \frac{n}{4}v_{\mathrm{A}}(AC)+\frac{4-n}{4}v_{\mathrm{A}}(AD),\\
v_{\mathrm{B}}(C_nD_{4-n}) &= \frac{n}{4}v_{\mathrm{B}}(BC)+\frac{4-n}{4}v_{\mathrm{B}}(BD),\\
v_{\mathrm{C}}(A_nB_{4-n}) &= \frac{n}{4}v_{\mathrm{C}}(AC)+\frac{4-n}{4}v_{\mathrm{C}}(BC),\\
v_{\mathrm{D}}(A_nB_{4-n}) &= \frac{n}{4}v_{\mathrm{D}}(AD)+\frac{4-n}{4}v_{\mathrm{D}}(BD).
\end{aligned}
\tag{4}
$$

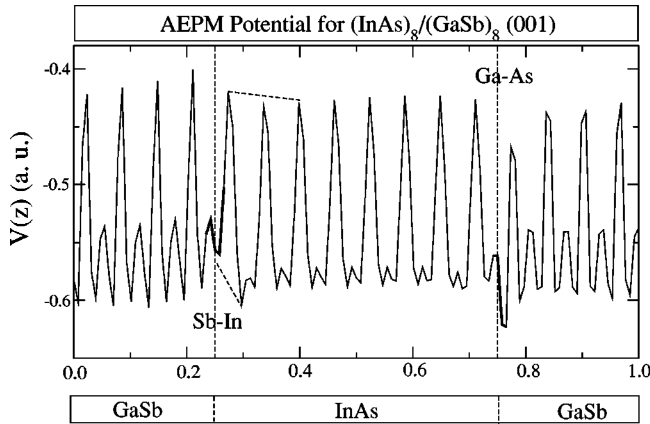

FIG. 3. Our atomistic semiempirical pseudopotential for the (001) $(InAs)_8/(GaSb)_8$ superlattice in atomic units. Note that the InAs potential is different for different InAs layers. Similarly, the two interfaces have different potentials (bold solid lines).

AC,BC,AD,BD are the four binary compounds, in our case GaSb, GaAs, InSb, and InAs, whose properties have been directly fitted to extract the atomic pseudopotential parameters. This procedure leads to a potential for the InAs monolayers closer to the interface different from the potential of the InAs monolayers in bulk InAs, in agreement with the results of more accurate self-consistent calculations. To test how this approximation works we show in Fig. 3 the potential obtained for $(InAs)_8/(GaSb)_8$ superlattice within our empirical pseudopotential approach. We see that the main features of the full *ab initio* potential are reproduced. The difference of the potential features at the two interfaces and the fact that the potential of the InAs layers closest to the interface is different from that relative to the layers in the bulk are an indication that *physical* features are introduced into the empirical approach.

An empirical pseudopotential calculation requires: (a) to determine a reliable equilibrium atomic configuration for the system and (b) to calculate the band structure relative to that given atomic configuration. To determine the atomic positions $R_{n\alpha}$ we minimize the elastic energy corresponding to a given atomic arrangement in the system, via the valence force field approach.[26] For (b) we expand the wave functions $\psi_i(r)$ in a plane-wave basis. The Hamiltonian matrix elements are calculated in this basis with no approximation, then the Hamiltonian matrix is diagonalized via the folded spectrum method.[27]

Our construction satisfies the conditions set for describing the electronic properties of no-common-atom SL's.

First, the use of atomic resolution in the potential [Eq. (3)] automatically allows for all (four) types of chemical bonds to be described.

Second, the superposition principle underlying Eq. (4) naturally allows for the potential of the various InAs monolayers to differ from each other, depending on their distance from the interface.

Third, the form factors $V(\mathbf{q}\neq\mathbf{G}_{BK})$ are determined *explicitly* by fitting many properties of bulk materials at different volumes and do not rely on some unknown numerical interpolation and extrapolation schemes.

Fourth, in our scheme the interdiffused interfaces can be described in a direct simple way without the need to introduce additional fitting parameters.

A demanding test of the ability of our scheme to describe systems whose atoms have a very different environment with respect to those of the fitted bulk compounds is the prediction of the band bowing of the four ternary random alloys $In_xGa_{1-x}As$, $In_xGa_{1-x}Sb$, $GaAs_{1-x}Sb_x$, and $InAs_{1-x}Sb_x$. The random alloys are modeled by occupying randomly the sites of a 512-atom cubic supercell. For each alloy configuration, the atomic positions were relaxed using the valence force field method, while the supercell size is determined by a lattice constant given by the composition average of the lattice constants of the constituent binary compounds following the Vegard's law. The optical band bowings are correctly predicted to be positive, and in the case of the $InAs_{1-x}Sb_x$ ternary alloy, we find the absolute minimum gap around $x=0.5$ in good agreement with experiment.[23] We obtain the following bowing parameters: for the $In_{0.5}Ga_{0.5}As$ alloy a value $b=0.54$ [expt. 0.49, 0.61 (Ref. 23)], for the $In_{0.5}Ga_{0.5}Sb$ alloy $b=0.32$ [expt. 0.42 (Ref. 23)], and for the $InAs_{0.5}Sb_{0.5}$ alloy $b=0.72$ [expt. 0.67 (Ref. 2), 0.76 (Ref. 23)]. Only for the $GaAs_{0.5}Sb_{0.5}$ alloy the calculated bowing 0.53 is definitely smaller than the experimental value 1.0.[23] The other recently proposed EPM theories for InAs/GaSb (Refs. 16,19) have not yet given results for alloy's bowing parameters. Since we have fitted only the bulk compounds these results show us that our scheme is an appropriate one for applications to segregated superlattices.

IV. RESULTS: INCREASED BAND GAP WITH THICKER GaSb LAYER

We have applied our method to the prediction of the band-gap blueshift of $(InAs)_8/(GaSb)_n$ and $(InAs)_6/(GaSb)_n$ superlattices with increasing GaSb layer thickness n. The trend of the band gap with the width of the GaSb hole well was recently measured by photoluminescence and absorbance spectroscopy.[28] This result was unexpected on the basis of simple confinement reasoning. In fact one would expect that keeping the InAs electron well width fixed would leave the bound-electron state energies unchanged while, by increasing the GaSb hole well width, the energy of the heavy-hole state would increase (since its confinement into the GaSb layer is reduced as the well thickness n increases). Our calculation shows that this is indeed the behavior of the heavy-hole energy. However, we find that the band gap increases with increasing n because the electron state energy itself increases with increasing n (becoming more confined) at a faster rate than the heavy-hole state energy. We find that only for $n\geqslant 32$ monolayers (ML) the electron states in nearest InAs wells are truly decoupled. For smaller n values, the first electron states are not confined. As a consequence the coupling between electrons in adjacent wells pushes their energy (corresponding to their bonding combination) down. Figure 4 shows the squared amplitude of the first electron wave functions for $(InAs)_8/(GaSb)_{12}$, $(InAs)_8/(GaSb)_{24}$, and $(InAs)_8/(GaSb)_{40}$. We can see that the electron wave functions spill considerably into the GaSb barriers. If the thick-

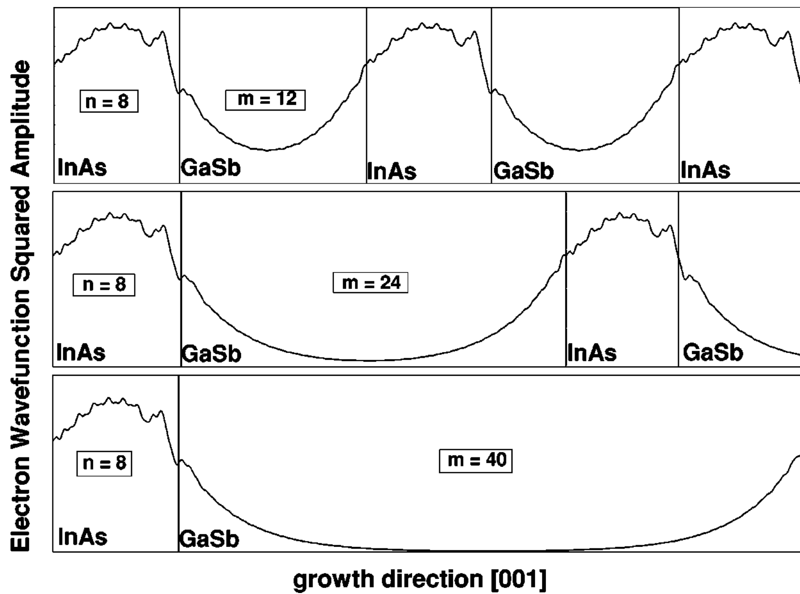

FIG. 4. Squared amplitude of the first electron wave functions of (a) $(InAs)_8/(GaSb)_{12}$, (b) $(InAs)_8/(GaSb)_{24}$, and (c) $(InAs)_8/(GaSb)_{40}$ (001) superlattices.

ness of the GaSb barrier is small, the electron wave functions overlap and extend along the growth direction.

The calculations have been performed both for superlattices with abrupt interfaces as well as for superlattices with interfacial disorder due to atomic segregation during growth. Some degree of interfacial segregation is always present in any real sample.[8] The effect of segregation has been modeled through a kinetic model of molecular-beam epitaxy growth. The details of our method for describing segregation are reported elsewhere.[12] We found that the band gaps of superlattices with segregated interfaces are always larger than the gaps calculated for the same nominal structures but assuming perfectly abrupt interfaces. We report our results for the $(InAs)_8/(GaSb)_n$ and $(InAs)_6/(GaSb)_n$ superlattices with abrupt interfaces in Fig. 5 comparing them with the results of other calculations, all using abrupt interfaces. In Fig. 6 we show our results for segregated superlattices obtained using the growth model with a growth temperature 380 °C and a deposition rate 0.5 ML/s, comparing them with the experimental data. The experimentally determined blueshifts were 70 meV (from absorbance measurements) and 75 meV (from photoluminescence measurements) for the $(InAs)_8/(GaSb)_n$ superlattices, while for the $(InAs)_6/(GaSb)_n$ superlattices, 102 meV and 107 meV were obtained, respectively.

A. Abrupt Interfaces: Comparison of different theories

Figure 5(a) shows the band gaps of abrupt $(InAs)_8/(GaSb)_n$ while Fig. 5(b) shows those of $(InAs)_6/(GaSb)_n$. We include in this figure only theories that assume abrupt interfaces, e.g., ours, the EPM of Dente

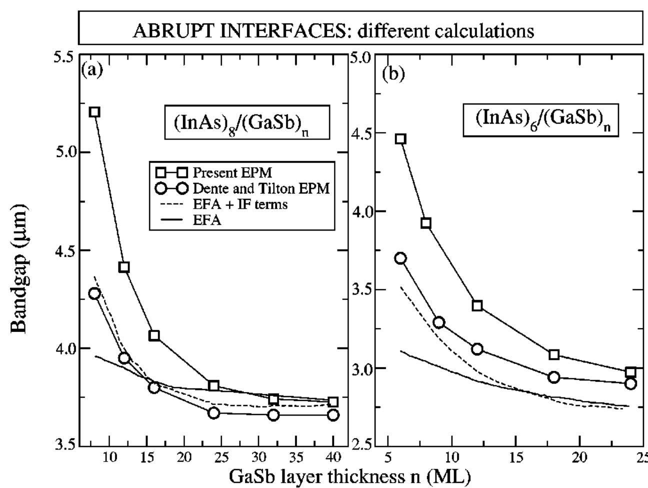

FIG. 5. (a) Comparison between the calculated band gaps of the $(InAs)_8/(GaSb)_n$ superlattice with abrupt interfaces: our EPM approach (empty squares), Dente and Tilton's EPM (empty circles), standard EFA (solid line), and EFA plus interface terms (dashed line) and (b) same for the $(InAs)_6/(GaSb)_n$ superlattice. The solid lines between symbols are drawn as a guide for the eye.

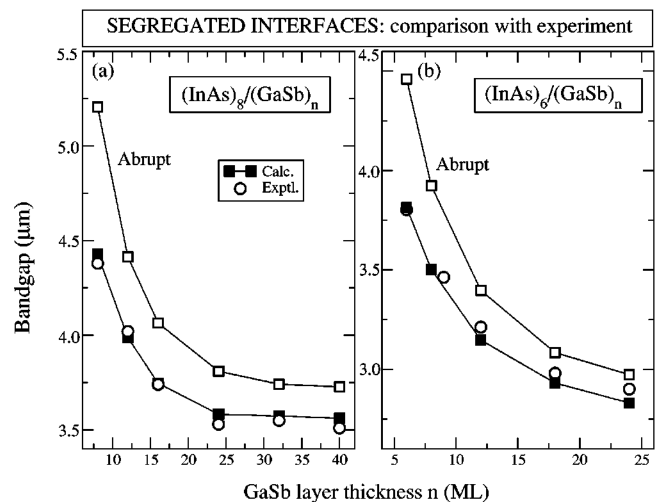

FIG. 6. Comparison between the results of our EPM approach for superlattices with abrupt interfaces (empty squares) and segregated interfaces (full squares) and the experimental data (empty circles): (a) $(InAs)_8/(GaSb)_n$ superlattices and (b) $(InAs)_6/(GaSb)_n$ superlattices.

and Tilton,[16] and two fourteen-band $\mathbf{k}\cdot\mathbf{p}$ calculations.[7] The calculations give the following values for the blueshifts of $n=8$: our EPM gives 95 meV, Dente and Tilton's EPM gives 49 meV, standard EFA gives 19 meV, EFA plus interface terms give 47 meV. The EPM theory of Ref. 20 while taking into account the effects of strain, when applied to the $(InAs)_{10}/(GaSb)_n$ superlattices (not measured yet) not only does not predict any blueshift of the band gap but finds a decreasing of the gap with increasing GaSb layer thickness n. We note the following.

(i) The two EPM calculations differ if the same (abrupt) geometry is assumed. The reason is the incomplete treatment of the interfaces by Dente and Tilton [factors (i)–(iv) outlined in Sec. II].

(ii) The standard $\mathbf{k}\cdot\mathbf{p}$ method hardly gives any blueshift. Only when interfacial potential terms are added,[9] fit to agree with the experimental data themselves, does one get the observed blueshift. However, the theory is not predictive since it requires an adjustable parameter to reproduce the data themselves.

The EPM calculations of Dente *et al.* and the $\mathbf{k}\cdot\mathbf{p}$ calculations of Lau *et al.*[7] assume that experiment can be fitted by using abrupt interfaces, even though interfacial interdiffusion is an observed fact. In contrast, we find that a proper theory does not fit experimental gaps if abrupt interfaces are assumed as shown next.

B. Interdiffused interfaces: Atomistic theory vs experiment

Figures 6(a) and 6(b) show $(InAs)_8/(GaSb)_n$ and $(InAs)_6/(GaSb)_n$ band gaps, respectively, comparing experiment, our interdiffused interfaces and our abrupt interfaces. Clearly, we can reproduce the experimental results (without any fit beyond that done for the bulk binaries) only if we use interdiffused interfaces.

Our theory is in very good agreement with the experimental data. Both the gaps of $(InAs)_8/(GaSb)_n$ and $(InAs)_6/(GaSb)_n$ superlattices with interdiffused interfaces were obtained using the same growth parameters in the kinetic model. These parameters, growth temperature 380 °C and a deposition rate 0.5 ML/s, are not too far from those used in the growth process (about 400 °C and a deposition rate 0.5 ML/s).[28] Our predicted band-gap blueshifts for the segregated superlattices are 68 meV for the $n=8$ case and 107 meV for the $n=6$ case, to be compared with the experimental values 70–75 meV for the $n=8$ case and 102–107 meV for the $n=6$ case.

V. SUMMARY

We have shown that our atomistic empirical pseudopotential for the InAs/GaSb quaternary system while fitted to only the binary compounds, is able to predict with sufficient accuracy trends in the interband transition energies of ideal and interdiffused superlattices and alloys. The scheme integrates the computational efficiency of the empirical plane-wave pseudopotential method with the description of both epitaxial and local strains and the details of potential changes over all the bonds in the quaternary system. The results have been compared with those of other recently proposed, but differently implemented, EPM theories.

ACKNOWLEDGMENTS

R.M. acknowledges support from EOARD through Grant No. FA8655-03-1-3017, while A.Z. acknowledges support from U.S.A. DOE, SC-BES-DMS.

[1] M.J. Yang, W.J. Moore, B.R. Bennet, and B.V. Shanabrook, Electron. Lett. **34**, 270 (1998); M.J. Yang, W.J. Moore, B.R. Bennet, B.V. Shanabrook, J.O. Cross, W.W. Bewley, C.L. Felix, I. Vurgaftman, and J.R. Meyer, J. Appl. Phys. **86**, 1796 (1999).
[2] I. Vurgaftman, J.R. Meyer, and L.R. Ram-Mohan, J. Appl. Phys. **89**, 5815 (2001).
[3] B.R. Bennett, B.V. Shanabrook, R.J. Wagner, J.L. Davis, J.R. Waterman, and M.E. Twigg, Solid-State Electron. **37**, 733 (1994).
[4] D. Gershoni, C.H. Henry, and G.A. Baraff, IEEE J. Quantum Electron. **29**, 2433 (1993).
[5] L.R. Ram-Mohan, K.H. Yoo, and R.L. Aggarwal, Phys. Rev. B **38**, 6151 (1988); L.R. Ram-Mohan and J.R. Meyer, J. Nonlinear Opt. Phys. Mater. **4**, 191 (1995).
[6] G.C. Dente and M.L. Tilton, J. Appl. Phys. **86**, 1420 (1999).
[7] W.H. Lau and M.E. Flatte', Appl. Phys. Lett. **80**, 1683 (2002).
[8] J. Steinshnider, M. Weimer, R. Kaspi, and G.W. Turner, Phys. Rev. Lett. **85**, 2953 (2000); J. Steinshnider, J. Harper, M. Weimer, C.H. Lin, S.S. Pei, and D.H. Chow, *ibid.* **85**, 4562 (2000).
[9] O. Krebs and P. Voisin, Phys. Rev. Lett. **77**, 1829 (1996); O. Krebs, D. Rondi, J.L. Gentner, L. Goldstein, and P. Voisin, *ibid.* **80**, 5770 (1998).
[10] S.H. Kwok, H.T. Grahn, K. Ploog, and R. Merlin, Phys. Rev. Lett. **69**, 973 (1993).
[11] R. Magri and A. Zunger, Phys. Rev. B **62**, 10 364 (2000).
[12] R. Magri and A. Zunger, Phys. Rev. B **64**, 081305 (2001).
[13] A. Zunger, Phys. Status Solidi A **190**, 467 (2002).
[14] R. Magri, L.L. Wang, A. Zunger, I. Vurgaftman, and J.R. Meyer, Phys. Rev. B **61**, 10 235 (2000).
[15] M.J. Shaw, P.R. Briddon, and M. Jaros, Phys. Rev. B **52**, 16 341 (1995).
[16] G.C. Dente and M.L. Tilton, Phys. Rev. B **66**, 165307 (2002).
[17] J.-B. Xia, Phys. Rev. B **39**, 3310 (1989).
[18] M.J. Shaw, Phys. Rev. B **61**, 5431 (2000).
[19] M.R. Kitchin, M.J. Shaw, E. Corbin, J.P. Hagon, and M. Jaros, Phys. Rev. B **61**, 8375 (2000); M.J. Shaw, E.A. Corbin, M.R. Kitchin, J.P. Hagon, and M. Jaros, J. Vac. Sci. Technol. B **18**, 2088 (2000).
[20] E. Corbin, M.J. Shaw, M.R. Kitchin, J.P. Hagon, and M. Jaros, Semicond. Sci. Technol. **16**, 263 (2001).
[21] M. Cohen and V. Heine, in *Solid State Physics*, edited by H. Ehrenreich, F. Seitz, and D. Turnbull (Academic Press, New York, 1970), Vol. 24 p. 64.

[22] P. Friedel, M.S. Hybertsen, and M. Schluter, Phys. Rev. B **39**, 7974 (1989).

[23] *Semiconductors: Group IV and III-V Compounds*, edited by O. Madelung, Landolt-Börnstein, New Series, Group III, Vol. 17 (Springer, Berlin, 1982); *Semiconductors: Intrinsic Properties of Group IV Elements and III-V, II-VI and I-VII Compounds*, edited by O. Madelung, Landolt-Börnstein, New Series, Group III, Vol. 22 (Springer, Berlin, 1987).

[24] S.-H. Wei and A. Zunger, Appl. Phys. Lett. **72**, 2011 (1998).

[25] R. Magri and A. Zunger, Phys. Rev. B **65**, 165302 (2002).

[26] P. Keating, Phys. Rev. **145**, 637 (1966).

[27] L.W. Wang and A. Zunger, J. Chem. Phys. **100**, 2394 (1994).

[28] R. Kaspi, C. Moeller, A. Ongstad, M.L. Tilton, D. Gianardi, G. Dente, and P. Gopaladasu, Appl. Phys. Lett. **76**, 409 (2000); A.P. Ongstad, R. Kaspi, C.E. Moeller, M.L. Tilton, D.M. Gianardi, J.R. Chavez, and G.C. Dente, J. Appl. Phys. **89**, 2185 (2001).

[29] D.M. Ceperley and B.I. Alder, Phys. Rev. Lett. **45**, 566 (1980).

[30] J.P. Perdew and A. Zunger, Phys. Rev. B **23**, 5048 (1981).